

# Resonantly diode laser pumped 1.6- $\mu\text{m}$ -erbium-doped yttrium aluminum garnet solid-state laser

Dmitri Garbuzov<sup>a)</sup> and Igor Kudryashov  
Princeton Lightwave Inc., 2555 US Route 130, Cranbury, New Jersey 08512

Mark Dubinskii  
U.S. Army Research Laboratory, AMSRD-ARL-SE-EO, 2800 Powder Mill Road, Adelphi, Maryland 20783

(Received 22 November 2004; accepted 22 February 2005; published online 25 March 2005)

We report direct resonant diode pumping of a 1.6- $\mu\text{m}$ -Er<sup>3+</sup>-doped bulk solid-state laser. Using a 1470-nm-single-mode diode laser module to pump the Er:YAG rod, an absorbed photon conversion efficiency of 26% has been obtained in this initial experiment. Analysis of the diode-pumped solid-state laser input–output characteristics suggests that the obtained slope efficiency can be doubled through the reduction of intracavity losses and pumping efficiency improvement. © 2005 American Institute of Physics. [DOI: 10.1063/1.1898427]

Recent progress in the development of quantum well separate confinement lasers based on the InGaAsP/InP system has been impressive.<sup>1–5</sup> Results reported in recent publications on 1.5- $\mu\text{m}$ -InGaAsP/InP diode arrays<sup>2–5</sup> as well as on individual multimode<sup>2</sup> and single mode emitters<sup>1</sup> have shown very promising performance improvements. For example, the output photon flux density, the key parameter for pumping applications, in the case of 40-W-1.5- $\mu\text{m}$ -diode arrays is 50% higher than that for commercial 50-W-0.9- $\mu\text{m}$ -GaAs-based arrays. An outstanding feature of InGaAsP/InP-based long-wavelength pumping sources is their excellent reliability with the potential for extremely long device lifetime ( $\sim 10^6$  h<sup>1,2</sup>). These results are paving the way for the development of a new generation of long-wavelength ( $> 1$   $\mu\text{m}$ ), eye-safe bulk solid-state lasers with resonance diode laser pumping. The yttrium aluminum garnet (YAG) crystal with low Er<sup>3+</sup> doping (to avoid upconversion losses<sup>6</sup>) is one of the most attractive active materials for such developments.

The known shortcomings of InP-based diodes as compared to GaAs diodes are reduced power conversion efficiency (30%) and higher temperature parameter sensitivity (the latter can be easily mitigated by advanced device temperature stabilization). Estimates show that reduced power conversion efficiency will be counterbalanced by increased optical-to-optical conversion efficiency in the ultralow-photon-defect “pump-lase” situation,<sup>2</sup> so that the overall efficiency of the InGaAsP/InP-diode-pumped Er-doped solid-state laser will be equal to or greater than that of the GaAs-diode-pumped version. A major advantage of the InGaAsP/InP-diode-pumped Er-doped solid-state laser is that the primary challenges of thermal management shift from the gain medium itself to the pumping diodes, thus greatly reducing thermal distortions deleterious to solid-state laser power scaling with diffraction-limited beam quality.

Spectroscopy of the 1450–1660 nm transitions between the <sup>4</sup>I<sub>13/2</sub> and <sup>4</sup>I<sub>15/2</sub> Stark-split manifolds in Er<sup>3+</sup>:YAG, forming a quasi-three-level system (Fig. 1), has been studied by numerous authors.<sup>7,8</sup> The four highest states derived from the eight Stark components of the ground <sup>4</sup>I<sub>15/2</sub> manifold can serve as the terminal states for Er<sup>3+</sup> laser transitions with

wavelengths ranging from 1617 to 1660 nm.<sup>6,8–11</sup> Published data for optical-to-optical efficiencies vary widely (from 2% to 3% up to 54%<sup>10</sup>) due to the essentially different “pump-lase” schemes, pumping source nature, and overall experimental conditions used.<sup>6,8–11</sup>

The results reported in this letter are the demonstration of direct resonant diode pumping of 1.6- $\mu\text{m}$ -Er<sup>3+</sup>-doped bulk solid-state lasers. To facilitate the onset of this new development, high-brightness cw single-mode InP-based diode lasers were used for pumping.<sup>1</sup> These 1470-nm-ridge waveguide lasers were packaged in standard telecom 12-pin-butterfly modules with polarization maintaining fiber output.

A 4.8-mm-long, 5-mm-diameter, Er<sup>3+</sup>(1%):YAG laser rod was single-end pumped in a folded polarization-coupled cavity as shown in Fig. 2. A polarizing beamsplitter cube was utilized to separate pumping and lasing radiation paths. A lens L1 and a high reflective mirror M1 (Fig. 1) provide appropriate pumping and laser mode geometric overlap with a beam waist radius of about 30  $\mu\text{m}$  in the rod center. Four different flat output couplers M<sub>2</sub> with transparencies of 0.24%, 3.3%, 9.4%, and 13.9% were used in these experiments.

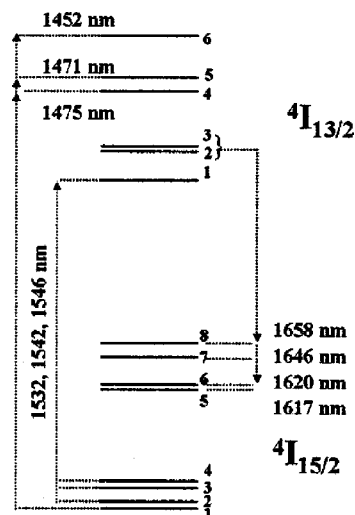


FIG. 1. Er<sup>3+</sup>:YAG absorptive and radiative transitions in the 1.45–1.66  $\mu\text{m}$  spectral range.

<sup>a)</sup>Electronic mail: dgarbuzov@princetonlightwave.com

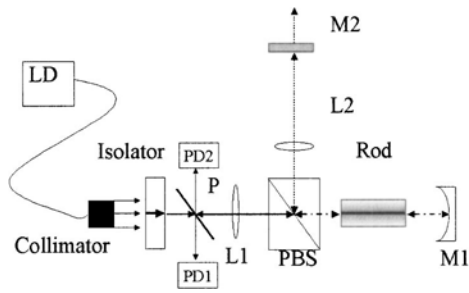


FIG. 2. Resonantly pumped Er<sup>3+</sup>:YAG (DPSSL) optical layout; (M<sub>1</sub>) plano-concave end mirror (30 mm ROC); (M<sub>2</sub>) plano-plano output coupler; (L<sub>2</sub>) Ar-coated intracavity lens; (P) diagnostic beam-splitter; (PD<sub>i</sub>) diagnostic photodiodes; (LD) fiber-coupled pumping laser diode (1470 nm).

Two photodiodes and a tilted glass plate (P) provide reference signals proportional to the incident and unabsorbed pump powers (Fig. 2). This data acquisition system was calibrated by signals taken with no rod in the cavity. As a result, the data acquisition system allowed for the effective double-path absorption coefficient ( $K_{\text{eff}}$ ) to be measured as well as to plot the solid-state laser output power as a function of the absorbed power. Our  $K_{\text{eff}}$  measurements indicate that  $K_{\text{eff}}$  decreases as the pump power increases and also depends on the output coupler transparency. In order to quantify these phenomena, the rod absorption measurements were performed using the broadband pumping radiation as a probe. Figure 3 shows absorption spectra in the vicinity of 1470 nm along with the pump module spectrum at the pump fiber end (output power about 300 mW). The pumping spectrum is broadened up to 12–14 nm due to the very high diode laser current density ( $>20$  kA/cm<sup>2</sup>). The absorption spectra in Fig. 3 are shown for the probe power at the laser threshold level ( $\sim 50$  mW, curve 2) as well as for the probe power level  $\sim 25$  times below the threshold (curve 1). Further reduction of the probe density does not change the absorption. The absorption reduction observed at high probe/excitation level (bleaching effect for curve 2 of Fig. 3) is taken into account during data acquisition. The bleaching effect also explains the fact that the absorption at a fixed incident power depends on the output coupler transparency (T). For optical couplers with higher transparency, the threshold is higher and the bleaching effect is stronger. At maximum incident

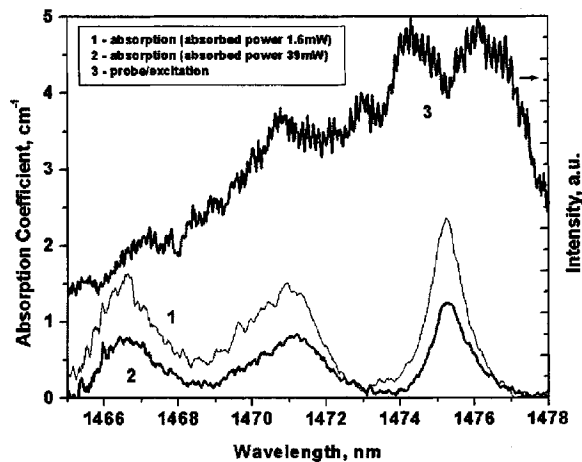


FIG. 3. (1) and (2) Absorption spectra (left scale) measured at low and “threshold” ( $\sim 50$  mW) excitation levels, respectively; (3) probe/excitation spectrum (right scale) of DL module.

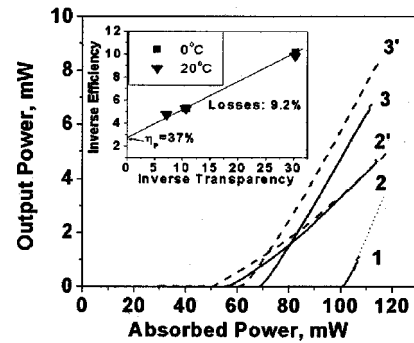


FIG. 4. Output power as a function of absorbed power for 1470-nm-pumped Er<sup>3+</sup>:YAG DPSSL with different output couplers: (1)  $T=13.9\%$ , (2) and (2')  $T=3.3\%$ ; (3) and (3')  $T=9.4\%$ . Curves 1, 2, and 3 were measured at rod temperature 0 °C and dashed curves (2'), and (3') at 20 °C. Values of absorbed photon conversion efficiency ( $\eta$ ) for curves (1), (2), and (2'), (3) and (3') are 26%, 9%, and 20%, correspondingly. Inset shows the inverse photon conversion efficiency ( $1/\eta$ ) vs inverse output coupler transmission.

power, the value of  $K_{\text{eff}}$  varies with coupler transparency from 45% at  $T=0.24\%$  to 38% at  $T=13.9\%$ . The increase in coupler transparency followed by the increase in threshold also leads to the output laser spectrum variation. At  $T=9.4\%$  and  $T=13.9\%$ , the DPSSL emits a single line at 1617 nm, while at  $T=3.3\%$  and  $T=0.23\%$ , the spectrum consists of two lines at 1617 and 1646 nm. Relative intensities of these lines do not change significantly with increasing pump power. The maximum power available from the pumping module was lower than that needed for lasing when  $T=13.9\%$  at  $T=20$  °C. The lasing with the 13.9% coupler was achieved only after the rod temperature was reduced to 0 °C (Fig. 4), and laser operation was restricted to only  $\sim 10\%$  above the threshold. Nevertheless, it was possible to estimate the absorbed photon conversion efficiency ( $\eta$ ) to be  $26\pm 3\%$  (Fig. 4). Corresponding values of  $\eta$  from the slope characteristics for  $T=3.3\%$  and  $9.4\%$  were 9% and 20%. These data have been incorporated into a loss and pumping efficiency analysis proposed by Caird.<sup>12</sup> By plotting data in the form of

$$\frac{1}{\eta} = \frac{1}{\eta_p} \left( 1 + \frac{L}{T} \right),$$

where  $T$  is the outcoupling loss value and  $\eta$  is the absorbed photon-to-photon conversion efficiency, intracavity losses of  $L=9.2\%$  and a pumping efficiency of  $\eta_p=0.37$  were inferred (inset of Fig. 4). The low value of  $\eta_p$  is clearly associated with imperfect pump and cavity physical active mode matching in this experiment. Another indication of low  $\eta_p$  is that the fluorescence intensity in nonlasing lines continues to grow with pumping rates above the threshold value. Double-path intracavity absorption losses in the polarizing beam-splitter at  $\lambda=1617$  nm were estimated to be  $\sim 8\%$ . Therefore, the total  $L$  value can be reduced by an order of magnitude so that  $\eta \cong \eta_p$ . The pumping efficiency can also be substantially improved, so that the slope efficiency can be essentially doubled.

In conclusion, we report the direct resonant diode pumping of a 1.6- $\mu\text{m}$ -Er<sup>3+</sup>-doped bulk solid-state laser. Using a 1470-nm-single-mode diode laser module to pump the Er:YAG rod, the absorbed photon conversion efficiency of 26% has been obtained in this experiment.

The authors acknowledge A. Kachanov and M. Itzler for creative discussions. This work was supported by the HEL-JTO/AF through the BAA Contract No. FA9451-04-C-0189.

- <sup>1</sup>D. Garbuzov, I. Kudryashov, A. Komissarov, M. Maiorov, W. Roff, and J. Connolly, in *Technical Digest of OFC 2003* (OSA, 2003), pp. 10–12.
- <sup>2</sup>D. Garbuzov and M. Dubinskii, in *Technical Digest of Solid State and Diode Lasers Technology Review, SSDLTR 2004* (Direct Energy Professional Society, 2004), p. 19.
- <sup>3</sup>G. Belenky, A. Gourevitch, D. Donetsky, D. Westerfeld, B. Laikhtman, C. W. Trussell, H. An, Z. Shellenbarger, and R. Martinelli, *Conference on Lasers and Electro-Optics 2003*, CLEO-2003 Technical Digest, CtuB2.
- <sup>4</sup>P. Crump, T. Crum, M. DeVito, J. Farmer, M. Grimshaw, Z. Huang, S. Igl, J. Wang, and W. Dong, *Technical Digest of SSDLTR 2004* (Direct Energy Professional Society), Diode-3.
- <sup>5</sup>R. Lammert, M. Osowski, M. Young, S. Oh, and J. Ungar, in *Technical*

- Digest of Solid State and Diode Lasers Technology Review, SSDLTR, 2004* (Direct Energy Professional Society), p. 10.
- <sup>6</sup>M. Iskandarov, A. Nikitichev, and A. Stepanov, *J. Opt. Technol.* **68**, 885 (2001).
- <sup>7</sup>N. Agladze, M. Popova, E. Vinogradov, T. Murina, and V. Zhekov, *Opt. Commun.* **65**, 351 (1988).
- <sup>8</sup>T. Schweizer, T. Jensen, E. Heumann, and G. Huber, *Opt. Commun.* **118**, 557 (1995).
- <sup>9</sup>K. Spariosu and M. Birnbaum, *IEEE J. Quantum Electron.* **30**, 1044 (1994).
- <sup>10</sup>Y. Young, S. Setzler, K. Snell, P. Budni, T. Pollak, and E. Chicklis, *Opt. Lett.* **29**, 1075 (2004).
- <sup>11</sup>H. Stange, K. Petermann, G. Huber, and E. Duczynski, *Appl. Phys. Lett.* **49**, 269 (1989).
- <sup>12</sup>J. Caird, S. Payne, P. Staver, A. Ramponi, L. Chase, and W. Krupke, *IEEE J. Quantum Electron.* **QE-24**, 1077 (1988).